

A basic helix-loop-helix transcription factor *DvIVS* determines flower color intensity in cyanic dahlia cultivars

Sho Ohno^{1*} · Ayumi Deguchi¹ · Munetaka Hosokawa^{1*} · Fumi Tatsuzawa² · Motoaki Doi¹

¹*Graduate School of Agriculture, Kyoto University, Sakyo-ku, Kyoto 606-8502, Japan*

²*Faculty of Agriculture, Iwate University, Morioka 020-8550, Japan*

*Corresponding author: Sho Ohno

Laboratory of Vegetable and Ornamental Horticulture, Graduate School of Agriculture, Kyoto University,
Sakyo-ku, Kyoto 606-8502, Japan

Telephone: +81-75-753-6048, Fax: +81-75-753-6068

E-mail: ono.sho.47n@st.kyoto-u.ac.jp

*Corresponding author: Munetaka Hosokawa

Laboratory of Vegetable and Ornamental Horticulture, Graduate School of Agriculture, Kyoto University,
Sakyo-ku, Kyoto 606-8502, Japan

Telephone: +81-75-753-6048, Fax: +81-75-753-6068

E-mail: mune@kais.kyoto-u.ac.jp

Ayumi Deguchi E-mail: a.deguchi@ax3.ecs.kyoto-u.ac.jp

Fumi Tatsuzawa E-mail: fumi@iwate-u.ac.jp

Motoaki Doi E-mail: dmotoaki@kais.kyoto-u.ac.jp

Abstract

The study was aimed to identify the factors that regulate the intensity of flower color in cyanic dahlia (*Dahlia variabilis*), using fifteen cultivars with different color intensities in their petals. The cultivars were classified into three groups based on their flavonoid composition: ivory white cultivars with flavones; purple and pink cultivars with flavones and anthocyanins; and red cultivars with flavones, anthocyanins, and chalcones. Among the purple, pink, and ivory white cultivars, an inverse relationship was detected between lightness, which was used as an indicator for color intensity and anthocyanin content. A positive correlation was detected between anthocyanin contents and the expression of some structural genes in the anthocyanin synthesis pathway that are regulated by *DvIVS*, a basic helix-loop-helix transcription factor. A positive correlation between anthocyanin content and expression of *DvIVS* was also found. The promoter region of *DvIVS* was classified into three types, with cultivars carrying Type 1 promoter exhibited deep coloring, those carrying Type 2 and/or Type 3 exhibited pale coloring, and those carrying Type 1 and Type 2 and/or Type 3 exhibited medium coloring. The transcripts of the genes from these promoters encoded full length predicted proteins. These results suggested that the genotype of the promoter region in *DvIVS* is one of the key factors determining the flower color intensity.

Keywords

Anthocyanin, bHLH, Correlation analysis, Dahlia, Flower color intensity

Abbreviations

ANS	Anthocyanidin synthase
bHLH	Basic helix-loop-helix
CHI	Chalcone isomerase
CHS	Chalcone synthase
DFR	Dihydroflavonol 4-reductase
F3H	Flavanone 3-hydroxylase
FNS	Flavone synthase
HPLC	High performance liquid chromatography

Introduction

Color is one of the most important characters of ornamental traits in flowers, and breeders strive to develop new exotic colors each day. Flower color results due to accumulation of secondary metabolites such as flavonoids including anthocyanins, carotenoids, and/or betalains. Generally, higher amounts of pigments deepen color intensity (Grotewold, 2006, Tanaka *et al.*, 2008). Inversely, lower pigment amounts in pigmented organs lead to paler coloring in carnation (*Dianthus caryophyllus*), eustoma (*Eustoma grandiflorum*), delphinium (*Delphinium*), and pelargonium (*Pelargonium × domesticum*) (Mato *et al.*, 2001, Uddin *et al.*, 2004, Hashimoto *et al.*, 2000, Fujioka *et al.*, 1991). In some cases, other factors such as cell shape and vacuolar pH strongly influence the flower color intensity (Mol *et al.*, 1998).

Garden dahlia (*Dahlia variabilis*) is one of the most popular ornamental plants in the world. In particular, dahlia has more abundant flower color variations than other floricultural species, with red, purple, pink, ivory white, and black cultivars resulting due to accumulation of anthocyanin, flavone, and/or butein derivatives (Takeda *et al.*, 1986, Nordström and Swain, 1953, Nordström and Swain, 1956, Nordström and Swain, 1958, Bate-Smith and Swain, 1953, Bate-Smith *et al.*, 1955, Harborne *et al.*, 1990, Price, 1939, Deguchi *et al.*, 2013). These flavonoids are synthesized in the flavonoid biosynthetic pathway, one of the most profusely studied plant secondary metabolite pathways. Flavonoids are initially synthesized in the phenylpropanoid synthesis pathway, and subsequently anthocyanins are synthesized in the anthocyanin synthesis pathway. Three molecules of malonyl-CoA and one molecule of 4-coumaroyl CoA are condensed by chalcone synthase (CHS), followed by chalcone isomerase (CHI), flavonoid 3-hydroxylase (F3H), dihydroflavonol 4-reductase (DFR), and anthocyanidin synthase (ANS) to synthesize anthocyanidin (Tanaka *et al.*, 2008). Transcription of some of these genes is promoted by a transcription complex composed of basic helix-loop-helix (bHLH), R2R3-MYB, and WD-repeat proteins (Koes *et al.*, 2005, Hichri *et al.*, 2011). The large variety of flower color in dahlias is presumably due to its genetic background. Garden dahlia is thought to be an autoallooctoploid with $2n = 8x = 64$ (Gatt *et al.*, 1998), and this complicated genetic background has led to the development of more than 50,000 cultivars in the past 100 years (McClaren, 2009). Highly polyploid species should offer more number of allelic combination and loci than diploid species, and correspondingly more complicated mechanisms are expected in the regulation of a given trait such as anthocyanin synthesis.

In a previous study (Ohno *et al.*, 2011a), we demonstrated that a bHLH transcription factor *DvIVS*, belonging to the subgroup of petunia *anthocyanin1* (Spelt *et al.*, 2000), *Arabidopsis thaliana* *TT8* (Nesi *et al.*, 2000), and common morning glory (*Ipomoea purpurea*) *IpIVS* (Park *et al.*, 2007), is associated with anthocyanin synthesis via regulation of *DvCHS1*, *DvF3H*, *DvDFR*, and *DvANS*, but not *DvCHS2* and *DvCHI* (Fig. 1). In another previous study (Ohno *et al.*, 2011b), due to absence of expression of *DvIVS* in commercial white (ivory white) cultivars derivatives of anthocyanidin were not produced. These results indicate that non-expression of both *DvIVS* and butein synthesis pathway genes

results in ivory white flowers, whereas expression of butein synthetic genes without the expression of *DvIVS* results in yellow flowers. In contrast, the expression of *DvIVS* without the expression of butein synthetic genes results in purple flowers, whereas expression of both *DvIVS* and butein synthetic genes results in red flowers. But there are paler color cultivars such as pink and orange cultivars in dahlia, and the mechanisms determining color intensity are unknown. We accordingly developed and tested a hypothesis that expression level of *DvIVS* determines the amount of anthocyanin and thereby flower color intensity. Because it is also likely that there are multiple *DvIVS* alleles in dahlia owing to its high polyploidy, we also investigated the involvement of a specific *DvIVS* genotype in the regulation of flower color intensity.

Materials and methods

Plant materials

We chose fifteen cultivars according to flower color: purple cultivars ‘Super Girl’, ‘Yukino’, ‘Cupid’, ‘Evelyn Rumbold’ and ‘Atom’; pink cultivars: ‘Magokoro’, ‘Jyunn-ai’ and ‘Saffron’; ivory white cultivars ‘Gitt’s Attention’, ‘Zannsetsu’, ‘Hakuba’ and ‘Hakuyo’; and red cultivars ‘Agitato’, ‘Nekkyu’ and ‘Red Velvet’ (Fig. 2a-o). Some cultivars were purchased from Akita International Dahlia Park (Akita, Japan). All cultivars were grown in the experimental farm of Kyoto University (Kyoto, Japan) and their petals were used for this study. For inverse PCR analysis, we used genomic DNA extracted from a red-white bicolor cultivar ‘Yuino’ (Ohno *et al.* 2011b).

Color analysis

Color components of the CIE $L^*a^*b^*$ co-ordinate were measured with the purpose of describing petal color differences of statistical significance. Color analyses were carried out following the Commission Internationale de l’Eclairage system. L^* indicates Lightness (black: 0 to white: 100). Positive a^* values indicate redness and negative a^* values indicate greenness. Positive b^* values indicate yellowness and negative b^* values blueness. Chroma (c^*), purity or saturation of the color, was calculated as follows: $c^* = (a^{*2} + b^{*2})^{1/2}$. The L^* , a^* , and b^* were measured with a hand held spectrophotometer (NR-3000, Nippon Denshoku Industries Co., Ltd., Tokyo, Japan). Three areas of the adaxial surface were subjected to color measurement. A mean score of the three replicate petals from three different flowers was calculated.

High performance liquid chromatography (HPLC) analysis

To determine the composition of flavonoids and anthocyanidins, HPLC analysis was performed according to Ohno *et al.* (2011a). In summary, petals were homogenized with acetic acid: methanol: water (1: 4: 5 v/v) solution for pigment extraction. The extracts were dried and re-dissolved in 2 mL of 20% hydrochloric acid. This solution was heated to evaporate the solvent, and 500 μ L of 20% hydrochloric acid was added to measure crude aglycons. HPLC analysis was performed using an LC10A system (Shimadzu, Kyoto, Japan) with a C18 column (Nihon Waters K.K., Tokyo, Japan) maintained at 40°C and a photodiode array detector. The detection wavelength was 350 nm for flavone and chalcone aglycones and 530 nm for anthocyanin aglycones.

Anthocyanin measurement

For anthocyanin quantification, 100 – 200 mg of fresh petals were homogenized in liquid nitrogen and 1 mL of extraction buffer (acetic acid: methanol: water = 1: 4: 5 v/v) was added. The extracted samples were centrifuged for 2 min at 20,600 \times g and the supernatant was collected. The supernatant was diluted 10 or 100 fold with the extraction buffer and the absorption at 520 nm was measured using a double beam spectrophotometer (U-2000A, Hitachi, Tokyo, Japan). The anthocyanin amount per 100 mg of fresh petals was recorded. A standard curve was prepared using cyanidin chloride (Polyphenols, Norway). The assay was performed with three petals from three independent inflorescences.

Other characteristics of petals

The pH of the petals was measured using previously described methods (Quattrocchio *et al.*, 2006). Petals (200 mg) were ground in 6 mL of distilled water. The pH was directly measured with a pH meter within 1 min. A mean of the three values was used for further data analysis.

To determine whether pigments were accumulating only in epidermal cells, fresh sections of ray florets were observed using a VHX-100 digital microscope (KEYENCE, Osaka, Japan). Epidermis cell structures were examined in resin sections prepared as follows. Petals were fixed in an FAA (ethanol: water: formalin: acetic acid, 12: 6: 1: 1 v/v) solution and cut into 5 mm squares. Samples were dehydrated in a graded ethanol series, and subsequently exchanged for Technovit 7100 resin (Heraeus Kulzer, Wehrheim, Germany) by immersing the samples in liquid resin for more than 3 h. Samples were solidified in the resin according to the manufacturer's protocol. The embedded samples were cut into 5 μ m sections using a motorized rotary microtome (RM2155, Leica, Wetzlar, Germany). Sections were stained with a 0.05% toluidine blue solution for 30 min and washed with water for 5 min. The dyed sections were observed and photographed with a VHX-100 digital microscope (KEYENCE).

Real-time RT-PCR

Total RNA was extracted with Sepasol[®]-RNA I Super G (Nacalai Tesque, Kyoto, Japan), purified with High-Salt Solution for Precipitation (Takara Bio Inc., Ohtsu, Japan), and reverse transcribed with ReverTra Ace (TOYOBO, Osaka, Japan), and 2 μ L of 50-fold diluted RT product was used as template for real-time RT-PCR. Real-time RT-PCR was performed with SYBR[®] Premix Ex Taq[™] II (Takara Bio Inc.) according to the manufacturer's instructions using a 7900HT Fast Real-Time PCR System (Applied Biosystems, Foster City, CA, USA). The primers used are shown in Supplementary Table S1. The PCR program was set at 95°C for 10 s, followed by 40 cycles of 95°C for 10 s, 60°C for 30 s, and subsequent dissociation steps. Three technical replications for two biological replications were performed and *actin* was used for an internal standard.

Correlation analysis

Correlations between L* and anthocyanin amount, L* and vertical-horizontal ratio of epidermal cell shape, L* and petal pH, anthocyanin content and anthocyanin synthesis pathway genes, and anthocyanin synthesis genes and *DvIVS* expressions were calculated. All correlation analysis was performed by linear approximation method using Microsoft Excel.

Isolation of *DvIVS* promoter region

The promoter region of *DvIVS* was isolated by inverse PCR. Genomic DNA of 'Yuino' (Ohno *et al.* 2011b) petals was isolated using a modified cetyltrimethylammonium bromide method (Murray and Thompson, 1980) and purified with MagExtractor[™]-Plant Genome- (TOYOBO). One microgram of genomic DNA was digested with *Hind* III (TOYOBO) and enzymes were removed with phenol/chloroform/ isoamyl alcohol (25: 24: 1) (Nacalai Tesque). After ethanol precipitation, 200 ng of digested DNA, 350 U of T4 DNA ligase (Takara Bio Inc.), and 10 \times buffer were mixed and water was added to 20 μ L. The mixture was incubated at 16°C overnight and PCR was performed with LA Taq (Takara Bio Inc.) using 1 μ L of ligation product as a template in a 10 μ L volume. The PCR program was set at 94°C for 1 min, followed by 35 cycles of 98°C for 10 s, 55°C for 10 s, and 68°C for 15 min. Primers used in this PCR were IVS-113R and IVS-G1163F (Supplementary Table S2) designed for our reported sequence (AB601010). PCR products were cloned into pTAC-1 vectors using Dyna-Express TA PCR Cloning Kit (BioDynamics Laboratory Inc., Tokyo, Japan) and all sequencing was performed using a BigDye[®] Terminator v 3.1 Cycle Sequencing Kit and a 3100 Genetic Analyzer (Applied Biosystems).

Genotyping of *DvIVS* promoter and cDNA sequences

For genotyping of *DvIVS* promoter region, primers were designed according to isolated promoter region sequence as shown in Supplementary Table S3 and PCR was performed with Blend Taq polymerase (TOYOBO) through the following steps and subsequently sequenced: initial denaturation at 94°C for 2 min, 30 cycles of denaturation at 94°C for 30 s, annealing at 55°C for 30 s, and extension at 72°C for 1 min, and a final extension at 72°C for 4 min.

The *DvIVS* cDNAs in ‘Super Girl’, ‘Yukino’, ‘Cupid’, ‘Evelyn Rumbold’, ‘Atom’, ‘Magokoro’, ‘Jyunn-ai’ and ‘Saffron’ were amplified with Blend Taq polymerase (TOYOBO) using IVS Full-F and IVS Full-R primers. The PCR products were cloned and sequenced as described above, using primers shown in Supplementary Table S2 designed for our reported sequence (AB601010). Subsequently, primers were designed to detect the specific transcript (Supplementary Table S4) and were amplified by RT-PCR with KOD FX polymerase (TOYOBO) through the following steps: initial denaturation at 94°C for 2 min, 30 cycles of denaturation at 98°C for 10 s, annealing at 55°C for 30 s, and extension at 68°C for 2 min, and a final extension at 68°C for 5 min.

To amplify the combination of promoter and transcribed RNA types, PCR was performed using newly designed primers shown in Supplementary Table S4 and S5 with Blend Taq polymerase (TOYOBO) through the following steps: initial denaturation at 94°C for 2 min, 30 cycles of denaturation at 94°C for 30 s, annealing at 55°C for 30 s, and extension at 72°C for 2 min, and a final extension at 72°C for 10 min. Twelve primer combinations (3 promoter type × 4 mRNA types) were analyzed.

Results

Flavonoid compositions and color differences

As difference among cultivars with respect to the modification of anthocyanidins and flavones was not observed (data not shown), the hydrolyzed aglycones were analyzed. In ivory white cultivars, only flavones, apigenin, and luteolin were detected, whereas in pink and purple cultivars, cyanidin, and pelargonidin were detected in addition to flavones (Table 1). In red cultivars, flavones, anthocyanidins, and chalcones, isoliquiritigenin and butein were detected (Table 1). Sulfuretin (aurone) was undetected or detected only at trace levels in all cultivars (Table 1). To simplify the experiments, only purple, pink, and ivory white cultivars were used for further the study.

Because deeper color generally shows lower L* value, L* value was used as an indicator of flower color intensity. When the color characteristics of 12 cultivars were plotted with c* on the X axis

and L^* on the Y axis, they could be classified into three groups corresponding to their appearances (Fig. 3). Ivory white cultivars had the highest L^* and the lowest c^* value. In contrast, purple cultivars had the lowest L^* and the highest c^* value. Pink cultivars had intermediate values for both the indices.

Anthocyanin contents and pH measurement

The anthocyanin contents of the 12 cultivars are shown in Fig. 4a. Purple cultivars contained the highest, with ‘Super Girl’ and ‘Yukino’ containing exceedingly high amounts, 0.7–1.0 mg anthocyanin per 100 mg petals. Other purple cultivars (‘Cupid’, ‘Evelyn Rumbold’ and ‘Atom’) contained 0.3–0.4 mg per 100 mg petals. We accordingly designated the former as deep purple cultivars and the latter as purple cultivars. Pink cultivars had lower anthocyanin amounts than purple cultivars, with <0.1 mg. In ivory white cultivars, no anthocyanin was detected, which was consistent with the HPLC results (Table 1). An inverse relationship between L^* and anthocyanin content was observed among eight cyanic (deep purple, purple, and pink) cultivars (Fig. 4b), suggesting that anthocyanin content was the key factor determining flower color intensity (L^*) in these cultivars.

The petal pH of the cultivars examined was 4.9–5.8 (Supplementary Table S6). No significant correlation was detected between L^* and petal pH (data not shown), suggesting that petal pH does not contribute to L^* .

Observation of petal sections

Observation of sections of fresh petals showed that anthocyanin accumulated only in epidermis (Supplementary Fig. S1a–d). No characteristic morphology was observed in resin sections of the eight cultivars (Supplementary Fig. S1e–h). To confirm the correlation between L^* and the vertical–horizontal ratio was analyzed, but no significant correlation was detected ($r = -0.50$; Supplementary Fig. S1i).

Real-time RT-PCR analysis

In a previous study (Ohno *et al.*, 2011a), we isolated anthocyanin synthesis structural genes and bHLH transcription factor *DvIVS*, which regulates the expression of *DvCHS1*, *DvF3H*, *DvDFR*, and *DvANS*. In the real-time RT-PCR analysis of *DvCHS1*, *DvF3H*, *DvDFR*, and *DvANS*, comparatively high expression levels were measured in ‘Super Girl’ and ‘Yukino’ and little or no expression was detected in ivory white cultivars (Fig. 5). The same expression patterns were detected for *DvIVS* (Fig. 5). In contrast, high expressions were detected in ivory white cultivars for *DvCHS2* and *DvCHI* (Fig. 5). Other transcription factors, *DvMYB1*, *DvMYB2*, *DvR3MYB*, *DvDEL* and *DvWDR1* showed different expression patterns from *DvCHS1*, *DvF3H*, *DvDFR*, *DvANS* and *DvIVS* (Supplementary Fig. S2).

We performed correlation analysis to investigate the relationships among anthocyanin contents, anthocyanin synthesis structural gene expression, and *DvIVS* expression. The *r* values (correlation coefficient) between anthocyanin content and *DvCHS1*, *DvCHS2*, *DvCHI*, *DvF3H*, *DvDFR*, and *DvANS* expression were 0.97, 0.09, 0.15, 0.87, 0.69, and 0.90, respectively (Fig. 6a-f). The *r* values between *DvIVS* and *DvCHS1*, *DvCHS2*, *DvCHI*, *DvF3H*, *DvDFR*, and *DvANS* expression were 0.99, 0.10, 0.22, 0.96, 0.81, and 0.97, respectively (Fig. 7a-f). The *r* value between anthocyanin contents and *DvIVS* expression was 0.96 (Fig. 6g), showing that anthocyanin content and the expression of *DvIVS* were strongly and positively correlated. In contrast, the *r* values between anthocyanin content and *DvMYB1*, *DvMYB2*, *DvR3MYB*, *DvDEL*, and *DvWDR1* expression were 0.01, 0.41, 0.41, 0.32, and 0.39, respectively (data not shown).

Length polymorphisms in *DvIVS* promoter region

Because the expression levels of a gene are usually affected by its promoter region, we isolated the promoter region of *DvIVS*. Fragments of 253 bp upstream of the *DvIVS* mRNA transcription start site were isolated by inverse PCR using ‘Yuino’, and this obtained promoter sequence was subsequently named Type 2. When we designed primers and PCR was performed using cyanic cultivars, there were three length polymorphisms were detected. These three fragments were sequenced and named Type 1–3.

Type 1 promoter was detected in the deep purple and purple cultivars (‘Super Girl’, ‘Yukino’, ‘Cupid’, ‘Evelyn Rumbold’ and ‘Atom’) by using IVS-2F and IVS-113R primers (Fig. 8a). Type 2 promoter was detected in ‘Cupid’, ‘Evelyn Rumbold’, ‘Atom’, ‘Jyunn-ai’, ‘Saffron’ and ‘Hakuyo’ by using IVS-3F and IVS-113R primers (Fig. 8a). Type 3 promoter was detected in ‘Cupid’, ‘Magokoro’, and ‘Saffron’ by using IVS-4F and IVS-113R primers (Fig. 8a). Thus deep purple cultivars carried only Type 1 promoters, purple cultivars carried Type 1 and Type 2 or all three promoters, pink cultivars carried Type 2 and/or Type 3 promoter(s), and ivory white cultivars except for ‘Hakuyo’ carried none of the promoter types (Fig. 8a). Type 2 promoter had a 125 bp insertion just behind the IVS-2F primer sequence, and Type 3 had another 103 bp insertion just behind IVS-3F primer sequence instead of 40 bp Type 2 specific fragment (Fig. 8b). In the putative TATA-box region, Type 1 had TTAAGTAG, while Type 2 and Type 3 had TTAAATAG (Fig. 8c).

Analysis of *DvIVS* transcripts and combination with promoter region

To analyze the relationship between polymorphisms of *DvIVS* promoter region and *DvIVS* mRNA expression levels, *DvIVS* cDNA from all cyanic cultivars were sequenced. Four different *DvIVS* cDNA sequences were isolated and named mRNA-1 to mRNA-4 (AB787557–AB787560) based on the differences at amino acid positions 235–295 of the putative protein (Supplementary Fig. S3). All these

mRNAs might encode complete putative proteins.

To determine the expressing mRNA types in cyanic cultivars, RT-PCR was performed using type-specific primers for each mRNA (Supplementary Table S4). mRNA-1 was detected in the deep purple and purple cultivars (‘Super Girl’, ‘Yukino’, ‘Cupid’, ‘Evelyn Rumbold’ and ‘Atom’); mRNA-2 in ‘Yukino’, ‘Cupid’ and ‘Jyunn-ai’; mRNA-3 in ‘Magokoro’ and ‘Saffron’; and mRNA-4 in ‘Evelyn Rumbold’ and ‘Saffron’ (Table 2).

Further, promoter–mRNA combinations were investigated to confirm that Type 1 promoter actually encodes a functional protein using specific primers (Supplementary Table S5). Consequently, the combinations of Type 1 promoter–mRNA-1, Type 2 promoter–mRNA-2, Type 3 promoter–mRNA-3, and Type 2 promoter–mRNA-4 were inferred (Table 2). Type 1 promoter–mRNA-1 combination was detected in the deep purple and purple cultivars (‘Super Girl’, ‘Yukino’, ‘Cupid’, ‘Evelyn Rumbold’ and ‘Atom’); Type 2 promoter–mRNA-2 in ‘Cupid’ and ‘Jyunn-ai’; Type 3 promoter–mRNA-3 in ‘Magokoro’ and ‘Saffron’; and Type 2 promoter–mRNA-4 in ‘Evelyn Rumbold’ and ‘Saffron’ (Table 2). The coding region associated with ‘Atom’ and ‘Hakuyo’ Type 2 was not identified, but no full length *DvIVS* transcript for this promoter was detected, it was suggested this promoter might be non-functional. Although, the promoter region associated with ‘Yukino’ mRNA-2 and the coding region associated with ‘Cupid’ Type 3 promoter, were neither identified, all deeply colored (deep purple and purple) cultivars retained Type 1 promoter–mRNA-1 combination, suggesting this allele is important for high anthocyanin accumulation.

Discussion

Anthocyanin contents determine flower color intensities in cyanic dahlia cultivars

In this study, the factors determining the flower color intensity of cyanic dahlia cultivars were analyzed. Usually flower color is determined by pigment composition and amount. We could classify fifteen cultivars into three groups by flavonoid composition: cultivars with flavones, cultivars with flavones and anthocyanins, and cultivars with flavones, anthocyanins, and butein (Table 1). All commercial red cultivars belonged to the last group, indicating that the purple anthocyanin pigments and the yellow pigment butein confer red flower color, and were excluded from further analysis. The twelve cultivars containing anthocyanins and/or flavones were used for further studies.

Although no difference in flavonoid composition between deep purple, purple, and pink cultivars was observed, their L^* values as an indicator of flower color intensity were different (Fig. 3, Supplementary Table S6). Anthocyanin contents and L^* values of the twelve cultivars showed an inverse relationship (Fig. 4b), suggesting that the anthocyanin contents determined flower color intensities.

Pigments accumulated in epidermal cells of petals in all cultivars (Supplementary Fig. S1a-d). In the snapdragon (*Antirrhinum majus*) *mixta* mutant, cell shape is associated with flower intensity (Noda *et al.*, 1994). From a comparative observation of epidermal cell shape, no relationship was detected between flower color intensity and cell shape (Supplementary Fig. S1i), indicating that cell shape is not involved in flower color intensity in cyanic dahlias. In Japanese morning glory (*Ipomoea. nil*), an increase in vacuolar pH is correlated with bluish flower display (Yoshida *et al.*, 1995). In our study, no significant correlation between L* value and petal pH was detected (data not shown) suggesting that petal pH contributes little to flower color intensity. From these results, we concluded that the quantity of total anthocyanins was the principal factor determining flower color intensity in cyanic dahlia cultivars.

Quantitative levels of *DvIVS* transcripts correlate flower color intensity by regulating anthocyanin content

In general, anthocyanin synthesis is regulated by bHLH, MYB, and WDR transcription factors (Koes *et al.*, 2005). Overexpression of one of these transcription factors induced high accumulation of anthocyanin in the flower (Laitinen *et al.*, 2008, Pattanaik *et al.*, 2010, Bai *et al.*, 2011). In petunia, common morning glory and tobacco, bHLH transcription factors have been shown to be one of key factors for floral anthocyanin biosynthesis (Spelt *et al.*, 2000, Park *et al.*, 2007, Bai *et al.*, 2011). In dahlia, we reported a bHLH transcription factor *DvIVS* regulates anthocyanin synthesis (Ohno *et al.*, 2011a), and thus it was assumed that the expression levels of *DvIVS* determined flower color intensity in dahlia.

In the present study, expressions of *DvCHS1*, *DvF3H*, *DvDFR*, and *DvANS* were strongly co-ordinated with both anthocyanin content and the expression of *DvIVS* (Fig. 6a-f, 7a-f). A positive correlation between expression levels of *DvIVS* and anthocyanin content was detected (Fig. 6g). Similarly, in tepals of Asiatic hybrid lilies a positive correlation between anthocyanin content and *LhMYB12* was found (Yamagishi *et al.*, 2012). In addition, we analyzed expression levels of *DvMYB1* (AB601003), *DvMYB2* (AB601004), *DvR3MYB* (AB621921), *DvDEL* (AB601006), and *DvWDR1* (AB601007) which are highly homologous to anthocyanin-regulating transcription factors (Supplemental Fig. S2), but no significant correlation was detected between the expression levels of these transcripts and anthocyanin synthesis gene expression or anthocyanin content. We accordingly suggest that *DvIVS* determines the anthocyanin content via regulation of structural genes, thereby regulating intensity of flower color.

The genotype of the *DvIVS* promoter region corresponds to the expression levels of *DvIVS*

We could classify the twelve cultivars into four groups: deep purple cultivars with high anthocyanin content (‘Super Girl’ and ‘Yukino’), purple cultivars with moderate anthocyanin content (‘Cupid’, ‘Evelyn Rumbold’ and ‘Atom’), pink cultivars with low anthocyanin content (‘Magokoro’, ‘Jyunn-ai’ and ‘Saffron’), and ivory white cultivars without anthocyanin (‘Gitt’s Attention’, ‘Zannsetsu’, ‘Hakuba’

and 'Hakuyo') (Fig. 4a). The observation of higher expression levels of *DvIVS* in deep purple and purple cultivars carrying Type 1 promoter than in the other cultivars suggested that the genotype of promoter region of *DvIVS* is an important factor in flower color intensity. There was only one allele with Type 1 promoter (mRNA-1) and Type 3 promoter (mRNA-3), whereas there were at least three alleles with Type 2 promoter (mRNA-2, mRNA-4, and an unidentified nonfunctional allele). However, all *DvIVS* transcripts except for the unidentified one encoded a full-length predicted protein and retained the same bHLH domain (Supplementary Fig. S3). This finding suggests that high accumulation of anthocyanin resulted from the total quantity of *DvIVS* transcripts rather than from protein activity encoded by mRNA-1 and that the difference in expression levels of *DvIVS* was due to the difference in the promoter activity. If that inference is true, Type 1 promoter has a stronger activity than Type 2 or Type 3 promoters. Two hypotheses may account for the difference in promoter activity. First, a single nucleotide polymorphism was found in the putative TATA box of the promoter, which is believed to be important for the transcriptional activity. Type 1 promoter had TTAAGTAG, whereas Type 2 and Type 3 promoters had TTAAATAG upstream of the transcription initiation site (Fig. 8c). This G to A mutation is the probable cause of low expression. Second, the promoter region itself accounts for the differential expressions. The genomic structure of Type 2 and Type 3 promoter had insertions with respect to Type 1 promoter (Fig. 8b). The upstream region near the transcription initiation site is very important for its expression, thus the insertion lowers the expression of *DvIVS*.

There appeared to be at least two different non-functional alleles. The first allele was detected in 'Hakuyo,' which had a Type 2 promoter. 'Hakuyo' did not express full length transcripts (Ohno *et al.*, 2011b), but expressed the 5' untranslated region of *DvIVS* (data not shown). This observation indicated that some genomic rearrangement(s) in the coding region led this allele to non-functional. The second was an unidentified allele which other ivory white cultivars would have. Although, we cannot exclude the possibility that alleles act as a negative regulator such as *AtMYBL2* (Dubos *et al.*, 2008, Matsui *et al.*, 2008) and *CPC* (Zhu *et al.*, 2009), however, a part of coding region of *DvIVS* were detected from these ivory white cultivars' genome (data not shown), suggesting some genomic rearrangement(s), perhaps in the promoter region, might lead this allele to non-functional. Thereby, further study of the genomic structure of ivory white cultivars will be required to clear the non-functional *DvIVS* alleles.

A functional allele is important for berry color in grape species (*Vitis × labruscana* and *V. vinifera*); that is, berry skin color is determined by the number of functional haplotype in MYB A genes (Kobayashi *et al.*, 2002, Kobayashi *et al.*, 2005, Kobayashi, 2009, Azuma *et al.*, 2011). Although we could not identify the promoter region of mRNA-2 in 'Yukino', the observation that deep purple cultivars carried only the stronger *DvIVS* promoter, whereas purple cultivars carried a weaker promoter in addition to the stronger promoter, indicated that the functional combination of the *DvIVS* promoter region determines flower color intensity in dahlia. To confirm this theory, the number of alleles should be measured using a digital PCR. But at least, Type 1 promoter explains deep coloring, given that 23 of 55

tested cultivars or seedling lines carried Type 1 promoter and 22 of 23 cultivars showed deep coloring (purple, red or black) (Ohno *et al.*, unpublished data).

Genetic background for flower color of dahlia

Dahlias have one of the largest numbers of cultivars of any cultivated species. Not only flower shape and size, but color variation is very large, with combinations of these factors distinguishing thousands of cultivars. This rich variation may be due to its highly polyploidy genetic background. Genetic redundancy is one of the advantages of polyploid species (Comai, 2005); however, from a breeding perspective it may interfere with the rapid development of new cultivars with desirable traits.

In the 1920s and 30s, Lawrence and colleagues proposed four elements of dahlia flower color inheritance; A: pale anthocyanin, B: deep anthocyanin, I: ivory flavone, and Y: yellow flavone (butein) (Lawrence, 1929, Lawrence and Scott-Honcrieff, 1935). In their reports, B (deep anthocyanin) was dominant to A (pale anthocyanin). Applying these factors to cultivars used in this experiment, pink cultivars might carry only A and purple cultivars might carry B. Thus, it is expected that the weakly functioning *DvIVS* Type 2 and Type 3 might correspond to factor A and the strongly functioning *DvIVS* Type 1 might correspond to B, and that I might correspond to the non-functional *DvIVS* allele carried by ivory white cultivars. Yellow or red cultivars usually contain buteins as a yellow pigment, and cultivars without buteins contain neither butein nor its precursor, isoliquiritigenin. We have shown that anthocyanin synthesis and butein synthesis are mutually independent in dahlia (Ohno *et al.*, 2011a), thus the Y element might correspond to the chalcone reductase gene or its transcription regulation factor.

In this study, it is suggested that more than six *DvIVS* alleles are present in dahlia. Further analysis is required, but in view of the observation that cultivars carrying Type 1 promoter are almost all deeply colored cultivars, it is suggested that this Type 1 promoter–mRNA-1 allele is the allele responsible for deeply colored cultivars. The finding that the anthocyanin contents or flower color intensities in cyanic cultivars are determined by variation in only one gene, *DvIVS*, is an unexpected result. It is due to high polyploidy in dahlia that the *DvIVS* Type 1 promoter may have been unintentionally selected for breeding as a color regulation factor.

In conclusion, we suggest that the genotype of *DvIVS* acts as a key factor determining flower color intensity in dahlia by controlling anthocyanin content via the regulation of anthocyanin pathway genes. In many floricultural species, a change in flower color is caused by mutation in specific structural genes. However, due to the presence of genetic redundancy in highly polyploid plants such as dahlia, a mutation in one specific structural gene rarely affects its phenotype. With the ongoing elucidation of flower color regulation in various species, these results may be used for efficient breeding of highly polyploidy crops by marker-assisted selection or genetic modification.

Supplementary Data

Fig. S1 The observation of petal sections.

Fig. S2 Relative expression levels of *DvMYB1*, *DvMYB2*, *DvR3MYB*, *DvDEL*, and *DvWDR1*.

Fig. S3 Alignment of deduced amino acid sequences encoded by *DvIVS* mRNA-1 to mRNA-4.

Table S1. Primers used for real-time RT-PCR.

Table S2. Primers used for inverse PCR and transcript sequencing.

Table S3. Primers used for analyzing the *DvIVS* promoter type.

Table S4. Primers used for analyzing the *DvIVS* mRNA type.

Table S5. Primers used for analyzing the combination of promoter and mRNA type.

Table S6. Measurement of color hue and cellular pH.

Figure legends

Fig. 1 Simplified flavonoid synthesis pathways in dahlia according to Ohno *et al.* (2011a). The genes framed with a rectangle are regulated by bHLH transcription factor *DvIVS*. Accumulation of anthocyanins and flavones resulted in purple or pink; that of anthocyanins, flavones, and buteins in red; and that of flavones alone in ivory white flower color. Higher anthocyanin contents confer deeper color intensities. In black cultivars, only anthocyanins are accumulated (Deguchi *et al.*, 2013). Abbreviations: ANS, anthocyanidin synthase; CH3H, chalcone 3-hydroxylase; CHI, chalcone isomerase; CHR, chalcone reductase; CHS, chalcone synthase; DFR, dihydroflavonol 4-reductase; F3H, flavanone 3-hydroxylase; F3'H, flavonoid 3'-hydroxylase; FNS, flavone synthase

Fig. 2

Dahlia cultivars used in this experiment. The order of photos is the same as Table 1. **a:** 'Super Girl' **b:** 'Yukino' **c:** 'Cupid' **d:** 'Evelyn Rumbold' **e:** 'Atom' **f:** 'Magokoro' **g:** 'Jyunn-ai' **h:** 'Saffron' **i:** 'Gitt's Attention' **j:** 'Zannsetsu' **k:** 'Hakuba' **l:** 'Hakuyo' **m:** 'Agitato' **n:** 'Nekkyu' **o:** 'Red Velvet'

Fig. 3

Distribution of L* (Lightness) and c* (Chroma) values of petals in twelve cultivars carrying flavones or anthocyanins and flavones. Squares, triangles, circles, and stars indicate ivory white, pink, purple, and deep purple cultivars, respectively

Fig. 4

Anthocyanin content analysis by spectrophotometer. **a:** Anthocyanin contents of cultivars. **b:** Correlation between L* (Lightness) and the reciprocal of anthocyanin content. Squares, triangles, circles, and stars indicate ivory white, pink, purple, and deep purple cultivars, respectively

Fig. 5

Relative expression levels of *DvCHS1*, *DvCHS2*, *DvCHI*, *DvF3H*, *DvDFR*, *DvANS*, and *DvIVS*. The constitutively expressed gene for actin was used as internal standard. All plots are based on a value of unity for 'Yukino.' The data are shown as an average of two biological replications

Fig. 6

Correlation analysis between anthocyanin contents and expression of genes involved in anthocyanin synthesis (**a:** *DvCHS1*, **b:** *DvCHS2*, **c:** *DvCHI* **d:** *DvF3H*, **e:** *DvDFR*, **f:** *DvANS* and **g:** *DvIVS*). Each relative gene expression is shown in Fig. 5. Squares, triangles, circles, and stars indicate ivory white, pink, purple, and deep purple cultivars, respectively

Fig. 7

Correlation analysis between *DvIVS* and anthocyanin synthesis structural gene (**a:** *DvCHS1*, **b:** *DvCHS2*, **c:** *DvCHI*, **d:** *DvF3H*, **e:** *DvDFR* and **f:** *DvANS*) expression in Fig. 5. Squares, triangles, circles, and stars indicate ivory white, pink, purple, and deep purple cultivars, respectively

Fig. 8

Polymorphisms in the *DvIVS* promoter region. **a:** PCR polymorphisms in promoter region by IVS-113R and IVS-pro-2F, IVS-pro-3F, or IVS-pro-4F primers (Supplementary Table S3). **b:** Summary figure based on sequence of *DvIVS* promoter region. Type 1 is according to the sequence 'Super Girl', 'Yukino', 'Cupid', 'Evelyn Rumbold' and 'Atom.' Type 2 is according to the sequence 'Jyunn-ai', 'Saffron' and 'Hakuyo', and Type 3 is according to 'Magokoro'. **c:** The single-nucleotide polymorphism in the putative TATA-box region of *DvIVS*. All sequenced cultivars retained a polymorphism.

Fig. S1

The observation of petal sections. Representative fresh petal sections (**a-d**) and resin sections (**e-h**) of some cultivars are shown. **a, e:** 'Super Girl', **b, f:** 'Evelyn Rumbold', **c, g:** 'Jyunn-ai', **d, h:** 'Gitt's Attention'. Bars in **e-h** panels indicate 100 μ m. **i:** Correlation analysis between L* and vertical–horizontal ratio of cell shape. Squares, triangles, circles, and stars indicate ivory white, pink, purple, and deep purple cultivars, respectively

Fig. S2

Relative expression levels of *DvMYB1*, *DvMYB2*, *DvR3MYB*, *DvDEL*, and *DvWDRI*. The constitutively expressed gene for actin was used as internal standard. All plots are based on a value of unity for 'Yukino.' The data are shown as an average of two biological replications

Fig. S3

Alignment of deduced amino acid sequences encoded by *DvIVS* mRNA-1 to mRNA-4. The basic helix-loop-helix domain is shown below the black boxes.

References

- Azuma A, Udo Y, Sato A, Mitani N, Kono A, Ban Y, Yakushiji H, Koshita Y, Kobayashi S (2011) Haplotype composition at the color locus is a major genetic determinant of skin color variation in *Vitis × labruscana* grapes. *Theor Appl Genet* 122:1427-1438
- Bai Y, Pattanaik S, Patra B, Werkman JR, Xie CH, Yuan L (2011) Flavonoid-related basic helix-loop-helix regulators, NtAn1a and NtAn1b, of tobacco have originated from two ancestors and are functionally active. *Planta* 234:363-375
- Bate-Smith EC, Swain T, Nördstrom CG (1955) Chemistry and inheritance of flower colour in the Dahlia. *Nature* 176:1016-1018
- Bate-Smith EC, Swain T (1953) The isolation of 2',4,4'-trihydroxychalkone from yellow varieties of *Dahlia variabilis*. *Journal of the Chemical Society*: 2185-2187
- Comai L (2005) The advantages and disadvantages of being polyploid. *Nat Rev Gen* 6:836-846
- Deguchi A, Ohno S, Hosokawa M, Tatsuzawa F, Doi M (2013) Endogenous post-transcriptional gene silencing of flavone synthase resulting in high accumulation of anthocyanins in black dahlia cultivars. *Planta* 237: 1325-1335
- Dubos C, Le Gourrierec J, Baudry A, Huep G, Lanet E, Debeaujon I, Routaboul J-, Alboresi A, Weisshaar B, Lepiniec L (2008) MYBL2 is a new regulator of flavonoid biosynthesis in *Arabidopsis thaliana*. *Plant J* 55:940-953
- Fujioka M, Kato M, Kakihara F, Tokumasu S (1991) Anthocyanidin composition of petals in

- Pelargonium X domesticum* Bailey. J Jpn Soc Hortic Sci 59:823-831
- Gatt M, Ding H, Hammett K, Murray B (1998) Polyploidy and evolution in wild and cultivated Dahlia species. Ann Bot 81:647-656
- Grotewold E (2006) The genetics and biochemistry of floral pigments. Annu Rev Plant Biol 57:761-780
- Harborne JB, Greenham J, Eagles J (1990) Malonylated chalcone glycosides in Dahlia. Phytochemistry 29:2899-2900
- Hashimoto F, Tanaka M, Maeda H, Shimizu K, Sakata Y (2000) Characterization of cyanic flower color of Delphinium cultivars. J Jpn Soc Hortic Sci 69:428-434
- Hichri I, Barrieu F, Bogs J, Kappel C, Delrot S, Lauvergeat V (2011) Recent advances in the transcriptional regulation of the flavonoid biosynthetic pathway. J Exp Bot 62:2465-2483
- Kobayashi S (2009) Regulation of anthocyanin biosynthesis in grapes. J Jpn Soc Hortic Sci 78:387-393
- Kobayashi S, Goto-Yamamoto N, Hirochika H (2005) Association of VvmybA1 gene expression with anthocyanin production in grape (*Vitis vinifera*) skin-color mutants. J Jpn Soc Hortic Sci 74:196-203
- Kobayashi S, Ishimaru M, Hiraoka K, Honda C (2002) Myb-related genes of the Kyoho grape (*Vitis labruscana*) regulate anthocyanin biosynthesis. Planta 215:924-933
- Koes R, Verweij W, Quattrocchio F (2005) Flavonoids: A colorful model for the regulation and evolution of biochemical pathways. Trends Plant Sci 10:236-242
- Laitinen RAE, Ainasoja M, Broholm SK, Teeri TH, Elomaa P (2008) Identification of target genes for a MYB-type anthocyanin regulator in *Gerbera hybrida*. J Exp Bot 59:3691-3703
- Lawrence WJC, Scott-Honcrieff R (1935) The genetics and chemistry of flower colour in Dahlia: A new theory of specific pigmentation. Journal of Genetics 30:155-226
- Lawrence WJC (1929) The genetics and cytology of Dahlia species. Journal of Genetics 21:125-159
- Mato M, Onozaki T, Ozeki Y, Higeta D, Itoh Y, Hisamatsu T, Yoshida H, Shibata M (2001) Flavonoid biosynthesis in pink-flowered cultivars derived from 'William Sim' carnation (*Dianthus caryophyllus*). J Jpn Soc Hortic Sci 70:315-319

Matsui K, Umemura Y, Ohme-Takagi M (2008) AtMYBL2, a protein with a single MYB domain, acts as a negative regulator of anthocyanin biosynthesis in Arabidopsis. *Plant J* 55:954-967

McClaren B (2009) *Encyclopedia of DAHLIAS*. Timber Press, Portland

Mol J, Grofewold E, Koes R (1998) How genes paint flowers and seeds. *Trends Plant Sci* 3:212-217

Murray MG, Thompson WF (1980) Rapid isolation of high molecular weight plant DNA. *Nucleic Acids Res* 8:4321-4325

Nesi N, Debeaujon I, Jond C, Pelletier G, Caboche M, Lepiniec L (2000) The TT8 gene encodes a basic helix-loop-helix domain protein required for expression of DFR and BAN genes in Arabidopsis siliques. *Plant Cell* 12:1863-1878

Noda KI, Glover BJ, Linstead P, Martin C (1994) Flower colour intensity depends on specialized cell shape controlled by a Myb-related transcription factor. *Nature* 369:661-664

Nordström CG, Swain T (1958) The flavonoid glycosides of *Dahlia variabilis*. III. Glycosides from white varieties. *Arch Biochem Biophys* 73:220-223

Nordström CG, Swain T (1956) The flavonoid glycosides of *Dahlia variabilis*. II. Glycosides of yellow varieties Pius IX and Coton. *Arch Biochem Biophys* 60:329-344

Nordström CG, Swain T (1953) The flavonoid glycosides of *Dahlia variabilis*. Part I. General introduction. Cyanidin, apigenin, and luteolin glycosides from the variety "Dandy.". *Journal of the Chemical Society*:2764-2773

Ohno S, Hosokawa M, Hoshino A, Kitamura Y, Morita Y, Park K, Nakashima A, Deguchi A, Tatsuzawa F, Doi M, Iida S, Yazawa S (2011a) A bHLH transcription factor, *DvIVS*, is involved in regulation of anthocyanin synthesis in dahlia (*Dahlia variabilis*). *J Exp Bot* 62:5105-5116

Ohno S, Hosokawa M, Kojima M, Kitamura Y, Hoshino A, Tatsuzawa F, Doi M, Yazawa S (2011b) Simultaneous post-transcriptional gene silencing of two different chalcone synthase genes resulting in pure white flowers in the octoploid dahlia. *Planta* 234:945-958

Park KI, Ishikawa N, Morita Y, Choi JD, Hoshino A, Iida S (2007) A bHLH regulatory gene in the common morning glory, *Ipomoea purpurea*, controls anthocyanin biosynthesis in flowers, proanthocyanidin and phytomelanin pigmentation in seeds, and seed trichome formation. *Plant J*

49:641-654

Pattanaik S, Kong Q, Zaitlin D, Werkman JR, Xie CH, Patra B, Yuan L (2010) Isolation and functional characterization of a floral tissue-specific R2R3 MYB regulator from tobacco. *Planta* 231:1061-1076

Price JR (1939) The yellow colouring matter of *Dahlia variabilis*. *Journal of the Chemical Society*:1017-1018

Quattrocchio F, Verweij W, Kroon A, Spelt C, Mol J, Koes R (2006) PH4 of petunia is an R2R3 MYB protein that activates vacuolar acidification through interactions with basic-helix-loop-helix transcription factors of the anthocyanin pathway. *Plant Cell* 18:1274-1291

Spelt C, Quattrocchio F, Mol JNM, Koes R (2000) Anthocyanin1 of *Petunia* encodes a basic helix-loop-helix protein that directly activates transcription of structural anthocyanin genes. *Plant Cell* 12:1619-1631

Takeda K, Harborne JB, Self R (1986) Identification and distribution of malonated anthocyanins in plants of the compositae. *Phytochemistry* 25:1337-1342

Tanaka Y, Sasaki N, Ohmiya A (2008) Biosynthesis of plant pigments: Anthocyanins, betalains and carotenoids. *Plant J* 54:733-749

Uddin AFMJ, Hashimoto F, Miwa T, Ohbo K, Sakata Y (2004) Seasonal variation in pigmentation and anthocyanidin phenetics in commercial *Eustoma* flowers. *Sci Hortic* 100:103-115

Yamagishi M, Yoshida Y, Nakayama M (2012) The transcription factor LhMYB12 determines anthocyanin pigmentation in the tepals of Asiatic hybrid lilies (*Lilium* spp.) and regulates pigment quantity. *Mol Breed* 30:913-925

Yoshida K, Kondo T, Okazaki Y, Katou K (1995) Cause of blue petal colour. *Nature* 373:291

Zhu HF, Fitzsimmons K, Khandelwal A, Kranz RG (2009) CPC, a single-repeat R3 MYB, is a negative regulator of anthocyanin biosynthesis in *Arabidopsis*. *Mol Plant* 2:790-802

Tables

Table 1. Flavonoid compositions of petals used in this experiment

Cultivars	Petal colors	Chalcone		Aurone Sulfuretin	Flavone		Anthocyanidin	
		Isoliquiritigenin	Butein		Apigenin	Luteolin	Cyanidin	Pelargonidin
'Super Girl'	Deep purple	-	-	-	+	+	+	+
'Yukino'	Deep purple	-	-	-	+	+	+	+
'Cupid'	Purple	-	tr	-	+	+	+	tr
'Evelyn Rumbold'	Purple	-	-	-	+	+	+	+
'Atom'	Purple	-	tr	-	+	+	+	tr
'Magokoro'	Pink	tr	tr	-	+	+	+	+
'Jyunn-ai'	Pink	-	-	-	+	+	+	+
'Saffron'	Pink	-	-	-	+	+	+	+
'Gitt's Attention'	Ivory white	tr	tr	tr	+	+	-	-
'Zannsetsu'	Ivory white	-	-	-	+	+	-	-
'Hakuba'	Ivory white	-	-	-	+	+	-	-
'Hakuyo'	Ivory white	-	-	-	+	+	-	-
'Agitato'	Red	tr	+	-	+	+	+	+
'Nekkyu'	Red	+	+	-	+	+	+	+
'Red Velvet'	Red	+	+	-	+	+	+	+

+: detected, tr: trace detected -: not detected

Table 2 Putative promoter-mRNA combination inferred from PCR analyses

Cultivars	Deep purple		Purple			Pink			Ivory white			
	Super Girl	Yukino	Cupid	Evelyn Rumbold	Atom	Magokoro	Jyunn-ai	Saffron	Gitt's Attention	Zannsetsu	Hakuba	Hakuyo
Promoter type	1	○	○	○	○	—	—	—	—	—	—	—
	2	—	—	○	○	○	—	○	○	—	—	○
	3	—	—	○	—	—	○	—	○	—	—	—
mRNA type	1	○	○	○	○	—	—	—	—	—	—	—
	2	—	○	○	—	—	—	○	—	—	—	—
	3	—	—	—	—	—	○	—	○	—	—	—
	4	—	—	—	○	—	—	—	○	—	—	—
Promoter-mRNA combination	p1-m1	p1-m1	p1-m1 p2-m2	p1-m1 p2-m4	p1-m1 p2-x	p3-m3	p2-m2	p2-m4 p3-m3				p2-x
Putative		p?-m2	p3-m?									

Figures

Fig. 1

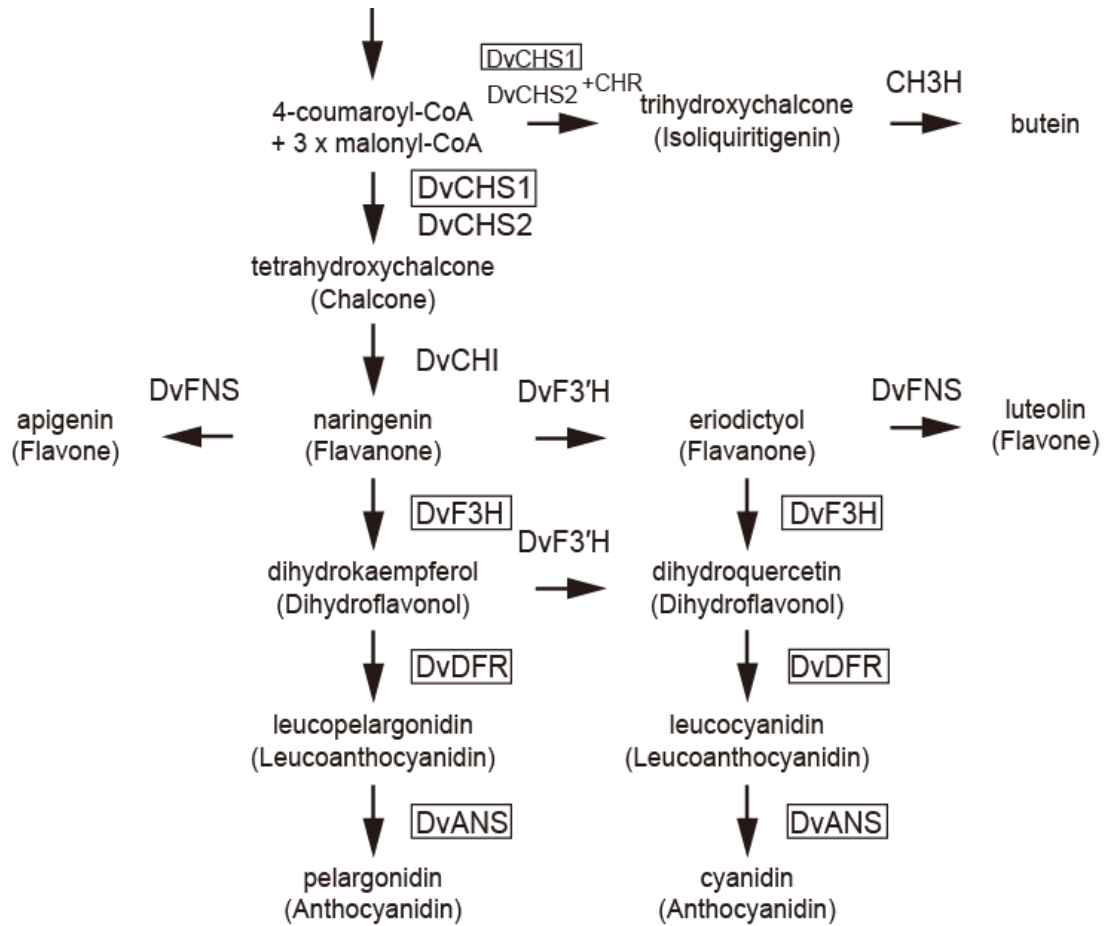


Fig. 2

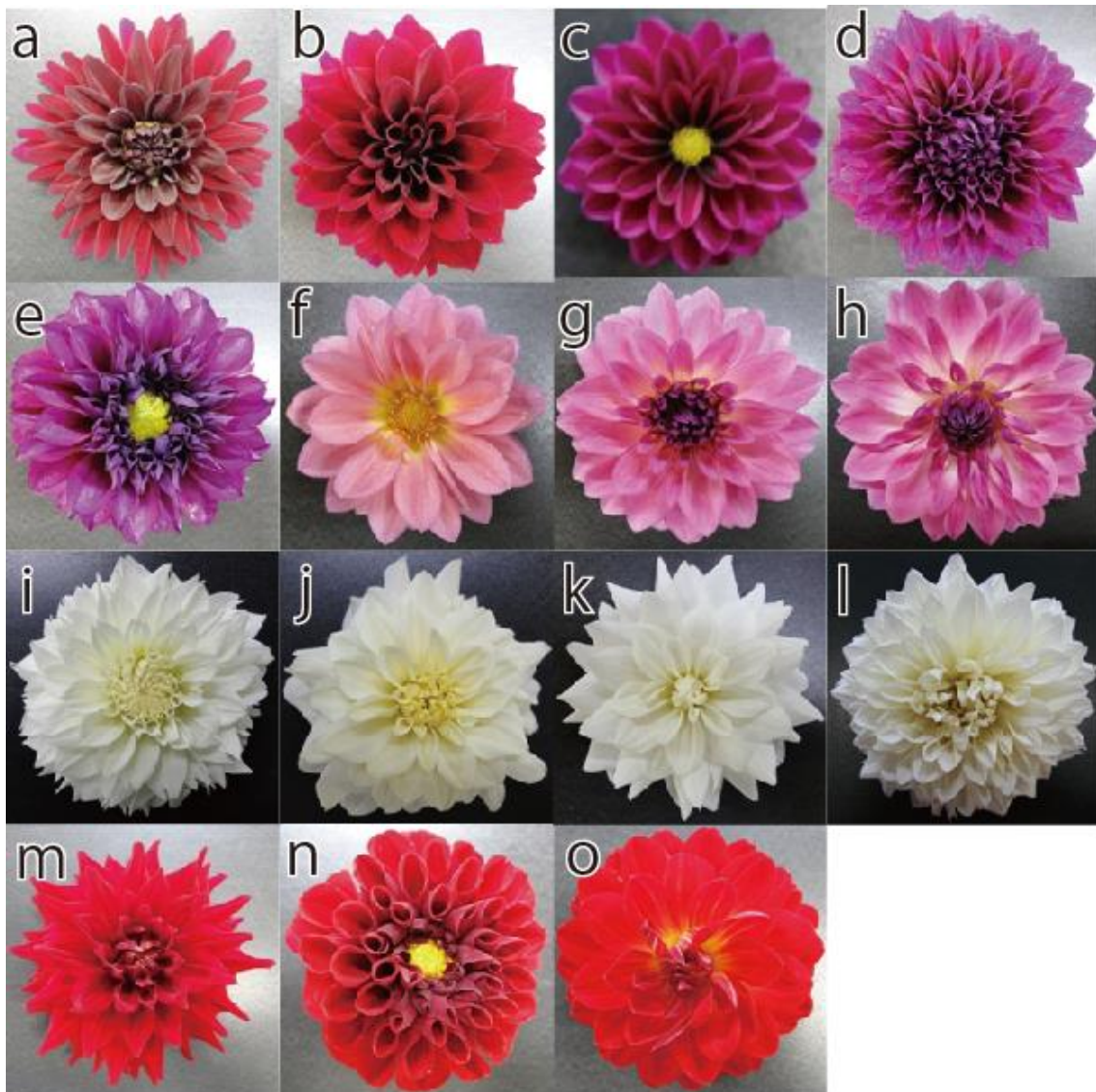


Fig. 3

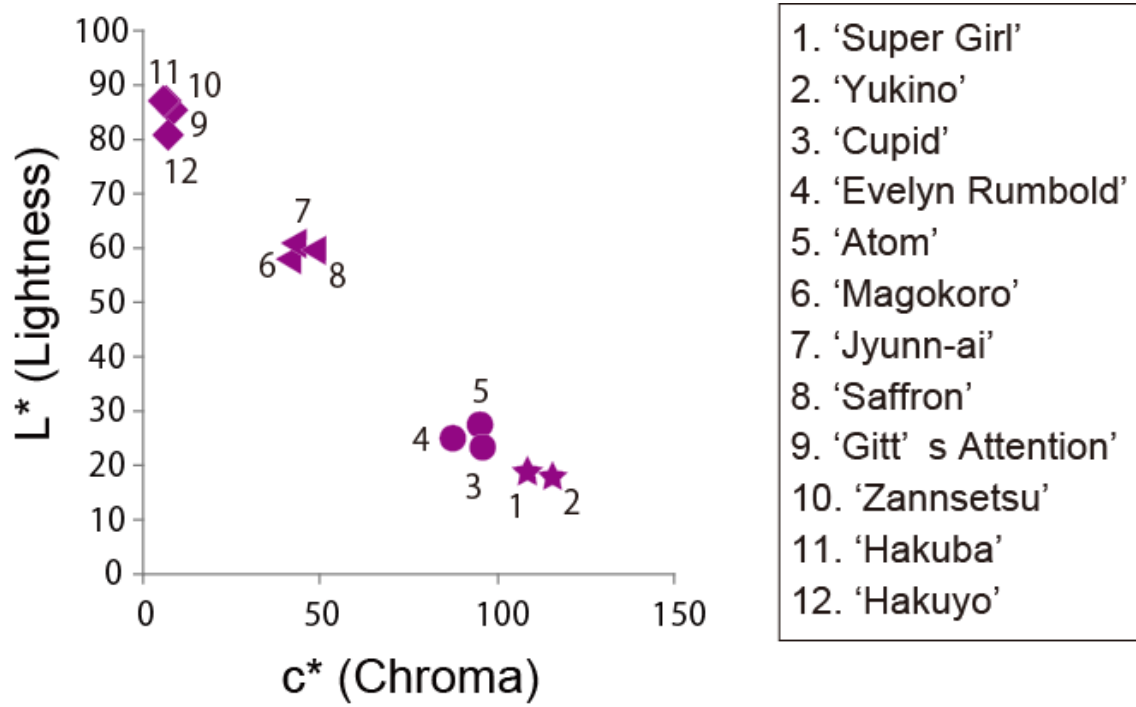


Fig. 4

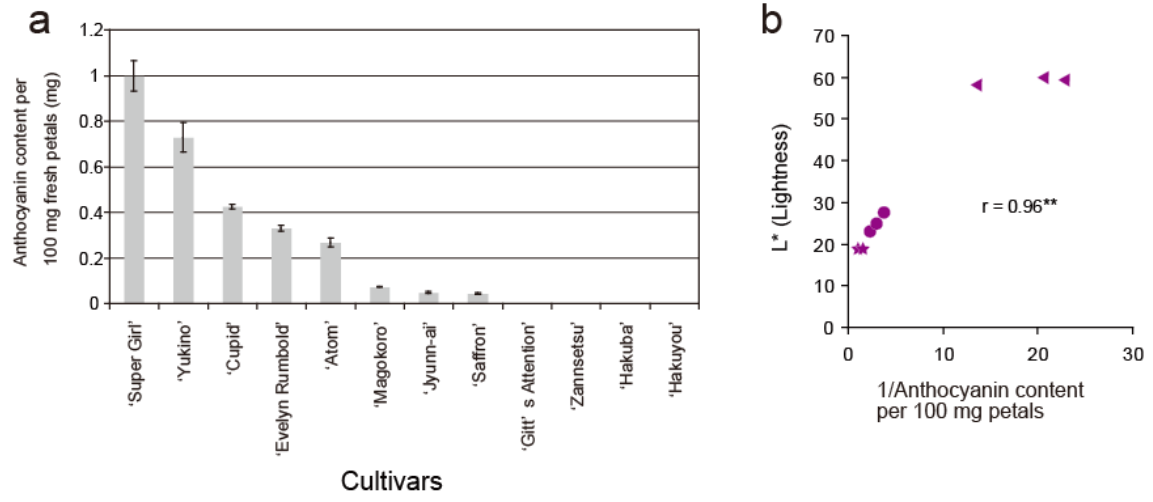


Fig. 5

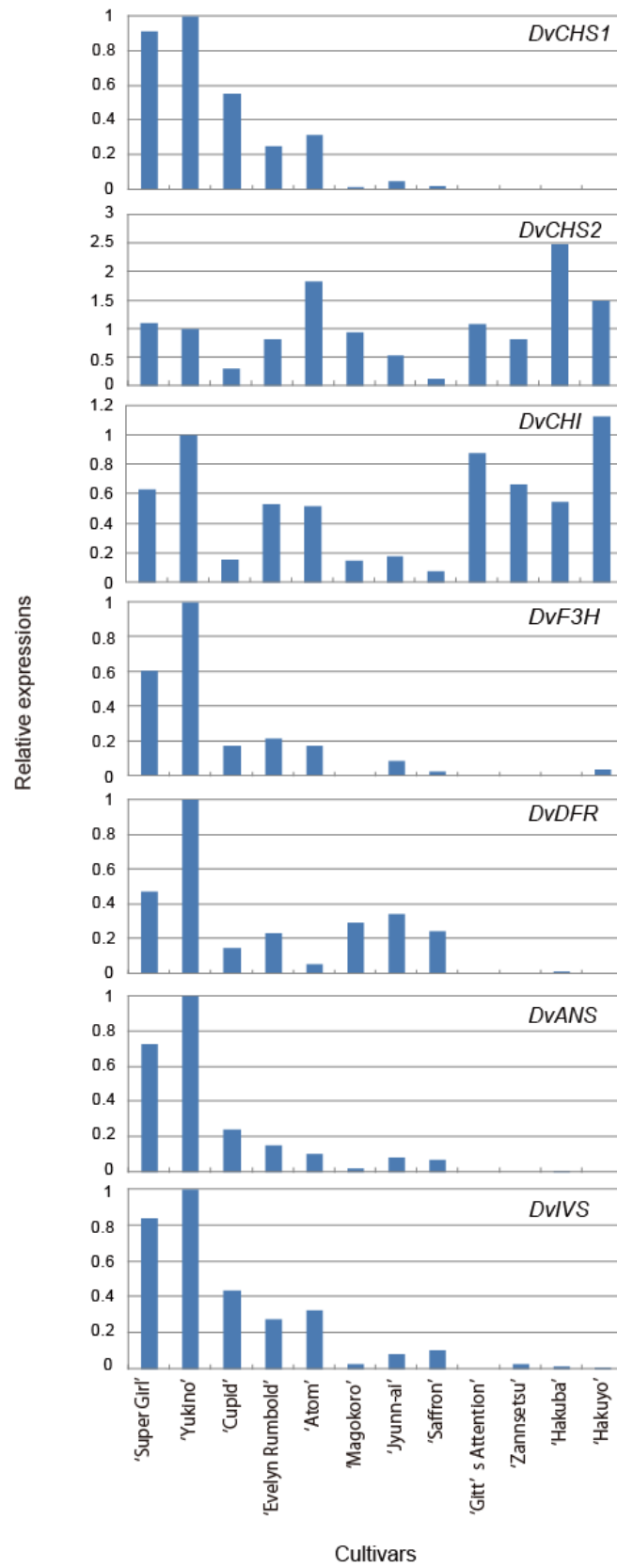


Fig. 6

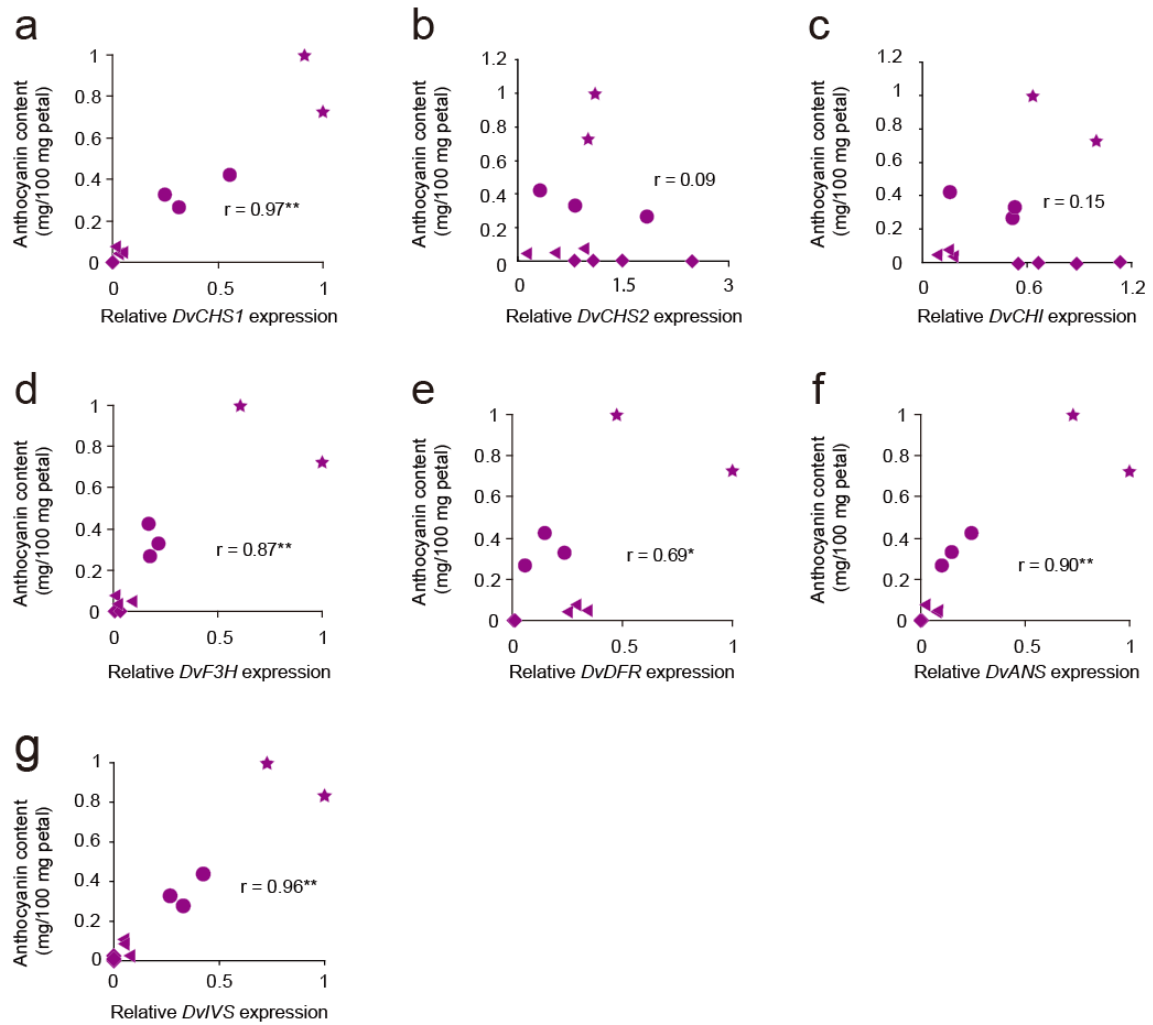


Fig. 7

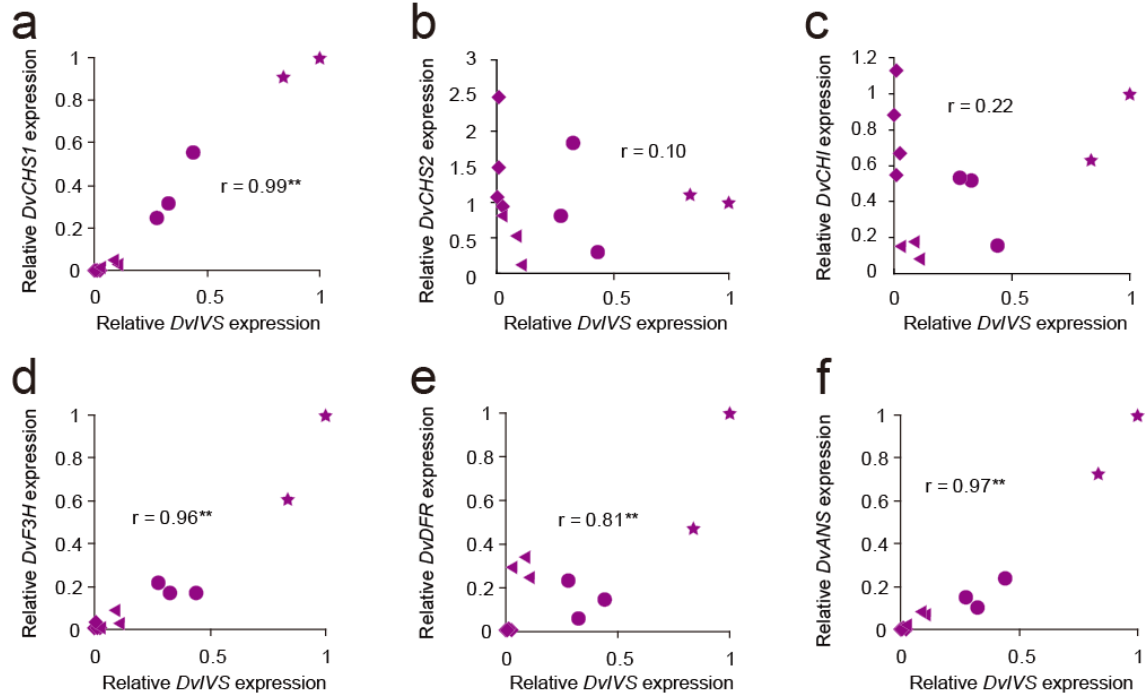
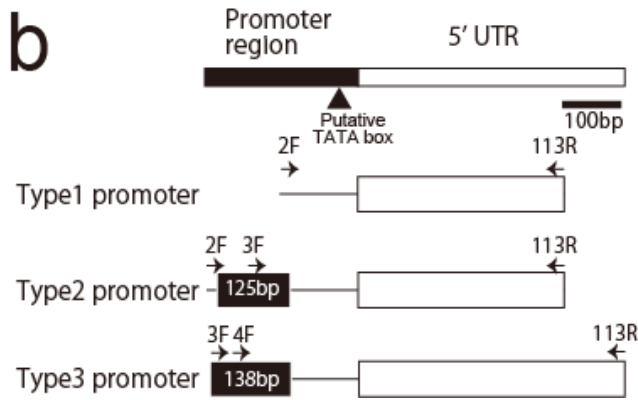
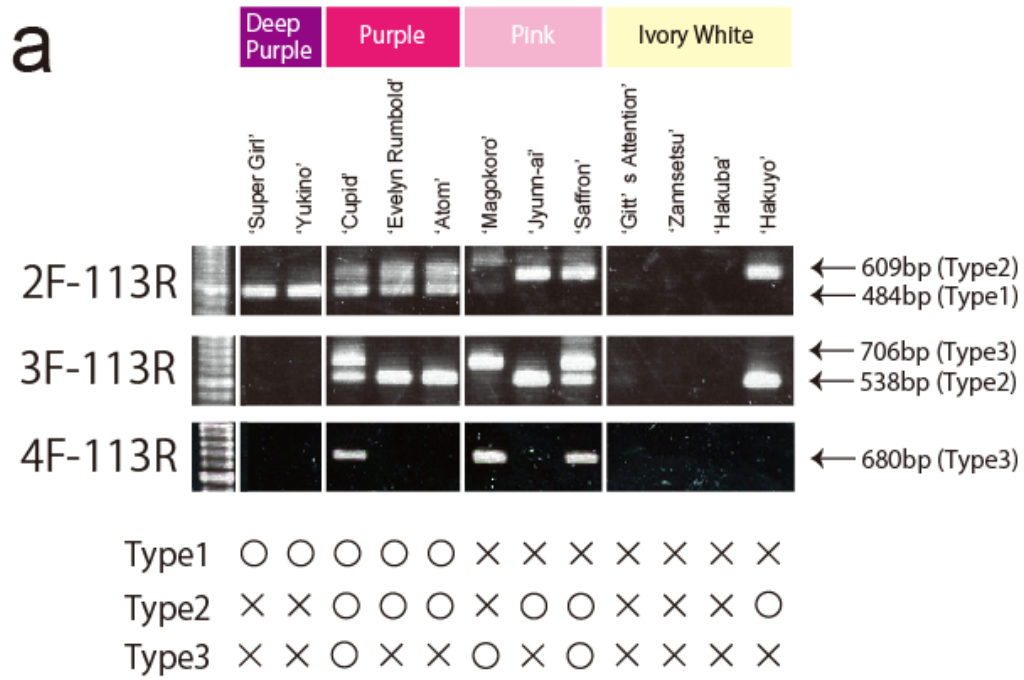


Fig. 8



c

TATAbox

Type1 promoter -33 TTAA**G**TAG -26

Type2 promoter -33 TTAA**A**TAG -26

Type3 promoter -33 TTAA**A**TAG -26

Supplemental tables

Table S1. Primers used for real-time RT-PCR

Genes	Forward Primers	Reverse Primers
<i>DvCHS1</i>	CATGTGCTAAGCGAATACGG	CCTCTCCGGTGGTATTGAAC
<i>DvCHS2</i>	TGTCCCAACTACCATGCCGATTTC	TTACACATTAATAATGACACAGTGA
<i>DvCHI</i>	AGAAGCTGGGAATGCAGTGT	GAGATCTGAGAGCCTTGATGC
<i>DvF3H</i>	TTGGAGGGAGATTGTGACCT	GGCCCATTAACCTCTTGCTA
<i>DvDFR</i>	CAACTTCCGGTCTATGACGAG	TTTCGGCCAATGTTTTTGAC
<i>DvANS</i>	GCTCCAACCTCTTCTACAACG	GAAATCCTGACCTTCTCCTT
<i>DvIVS</i>	CATAACCCAAGTAAAGAAAGCCATT	CATCCATTTTTAAATTGTTTGTGGT
<i>DvMYB1</i>	GTTCACTACTTTAGCAAACG	GACTTTGATATCAACCGGAT
<i>DvMYB2</i>	TTTGCTCTCCATAGATCAAC	GCCGTGAGTTCTAATATAAG
<i>DvR3MYB</i>	ATCAACCATTGACGATATCAACAAT	GATTTGTAAAAAGACTAATGATAA
<i>DvDEL</i>	ATCTAAGTTAAAGAGTTGTACAGC	TGAAACTTGGAAAATTGGACTCAA
<i>DvWDR1</i>	AGGCGTTGTGGAAACTCAAT	TTATCGCGAAGGTCGAAAAC
<i>DvActin</i>	TGCTTATGTTGGTGATGAAG	CCCTGTTAGCCTTAGGATTT

Table S2. Primers used for inverse PCR and transcript sequencing

	Primers	Objects
IVS-113R	TATTCGAATTTACAGTCAAATATTG	Inverse PCR
IVS-G1163F	TCCCAGCTCACGGTTCAGTTTTAAA	Inverse PCR
IVS-Full-F	TTTGACGTAATTTTGGACCTAATTT	Transcript sequencing
IVS-474F	CGGTGAGCAACAGGTGGCGGAGAA	Transcript sequencing
IVS-625F	GCATATGCAAAGCAGCAAGATCTAT	Transcript sequencing
IVS-725F	CGGTGATATGCATCCCTGTACTAAA	Transcript sequencing
IVS-826R	TGAAGAAAAGTTTCACATGTTGAAT	Transcript sequencing
IVS-1037F	GACGGACTTCATGAAAGAAACATA	Transcript sequencing
IVS-1082F	TGCCTCACAATAATAAAGATTCAAT	Transcript sequencing
IVS-1316F	CAGAAGAATTTGCACCGGAGTTTA	Transcript sequencing
IVS-1614R	GAGCTCTTCGTGCGACGTCGTTTT	Transcript sequencing
IVS-Full-R	CATCCATTTTTAAATTGTTTGTGGT	Transcript sequencing

Table S3. Primers used for analyzing the *Dv*IVS promoter type

Primer	Promoter type	Forward Primers	Reverse Primers
IVS-2F	Type 1 and 2	ATAATTTTCTTTTAAGTTACGGATT	
IVS-3F	Type 2 and 3	TTTGAGTTACAGAATTGATTGTGCT	
IVS-4F	Type 3	GCCGAATTGCGATTGGGGGGATT	
IVS-113R	All types		TATTCGAATTCACGTCAAATATTG

Table S4. Primers used for analyzing the *Dv*/VS mRNA type

mRNA type	Forward Primers	Reverse Primers
mRNA-1	GAAACAATAATGGCTGCCGCTGGTT	TCTTCTGCCTCATCATCATCGT
mRNA-2	GAAACAATAATGGCTGCCGCTGGTC	GCCTCATCACATCCTGCATCTTAC
mRNA-3	GAAGAAACAATAATGGCTGCTGACG	ACCCTCATCATCATCATCATCA
mRNA-4	GAAACAATAATGGCTGCCGCTGACG	TGCATCTTACCCTCATCATCT

Table S5. Primers used for analyzing the combination of promoter and mRNA type

	Forward Primers	Reverse Primers
Type 1 promoter	TTTCTTTTAAGTTACGGATTTTCGC	
Type 2 promoter	GTGCTGCCAGTAACCCCACGACTTT	
Type 3 promoter	GCCGAATTGCGATTGGGGGATT	
<i>Dv/VS</i> mRNA-1		CTTCAATCCGTCATCGTTTACGGA
<i>Dv/VS</i> mRNA-2		AACATCTCTTTCAATCCGTCATCA
<i>Dv/VS</i> mRNA-3		ACATCTCTTTCAATCCGTCAGCAG
<i>Dv/VS</i> mRNA-4		TCTCTTTCAATCCGTCAGCGGCAG

Table S6. Measurement of color hue and cellular pH

	L*	a*	b*	c*	pH
'Super Girl'	19.0 ± 0.3	107.8 ± 1.8	12.6 ± 0.6	108.5 ± 1.8	5.4 ± 0.0
'Yukino'	18.9 ± 0.7	114.1 ± 2.2	14.1 ± 0.5	115.0 ± 2.2	5.2 ± 0.0
'Cupid'	23.3 ± 1.4	96.0 ± 1.9	-1.4 ± 2.8	96.2 ± 1.8	5.4 ± 0.0
'Evelyn Rumbold'	24.9 ± 1.1	87.0 ± 2.5	-5.1 ± 3.7	87.4 ± 2.3	5.5 ± 0.0
'Atom'	27.5 ± 0.6	94.4 ± 1.6	-13.0 ± 0.5	95.3 ± 1.5	5.4 ± 0.0
'Magokoro'	58.1 ± 2.2	43.0 ± 3.2	0.61 ± 1.7	43.1 ± 3.1	not measured
'Jyunn-ai'	60.1 ± 1.9	43.3 ± 2.3	-10.6 ± 0.9	44.5 ± 2.4	5.8 ± 0.1
'Saffron'	59.5 ± 2.3	47.8 ± 2.7	-11.5 ± 0.2	49.2 ± 2.6	5.4 ± 0.0
'Gitt's Attention'	85.4 ± 0.7	-3.6 ± 0.3	7.4 ± 0.3	8.3 ± 0.5	5.8 ± 0.1
'Zannsetsu'	87.2 ± 0.6	-2.5 ± 0.3	6.0 ± 0.2	6.5 ± 0.3	5.5 ± 0.0
'Hakuba'	86.9 ± 0.4	-2.0 ± 0.1	5.3 ± 0.5	5.6 ± 0.5	5.5 ± 0.0
'Hakuyo'	80.9 ± 1.0	-3.3 ± 0.1	5.8 ± 0.5	6.7 ± 0.4	5.7 ± 0.0
'Agitato'	26.6 ± 1.2	88.9 ± 2.7	27.5 ± 1.6	93.1 ± 2.2	5.5 ± 0.0
'Nekkyu'	26.8 ± 0.5	92.2 ± 0.9	26.3 ± 0.9	95.9 ± 0.7	4.9 ± 0.0
'Red Velvet'	39.9 ± 2.9	73.0 ± 5.9	38.5 ± 1.2	82.8 ± 4.6	5.3 ± 0.0

The data shown indicates the mean ± S. E., $n = 3$ replicates.

Supplemental figures

Fig. S1

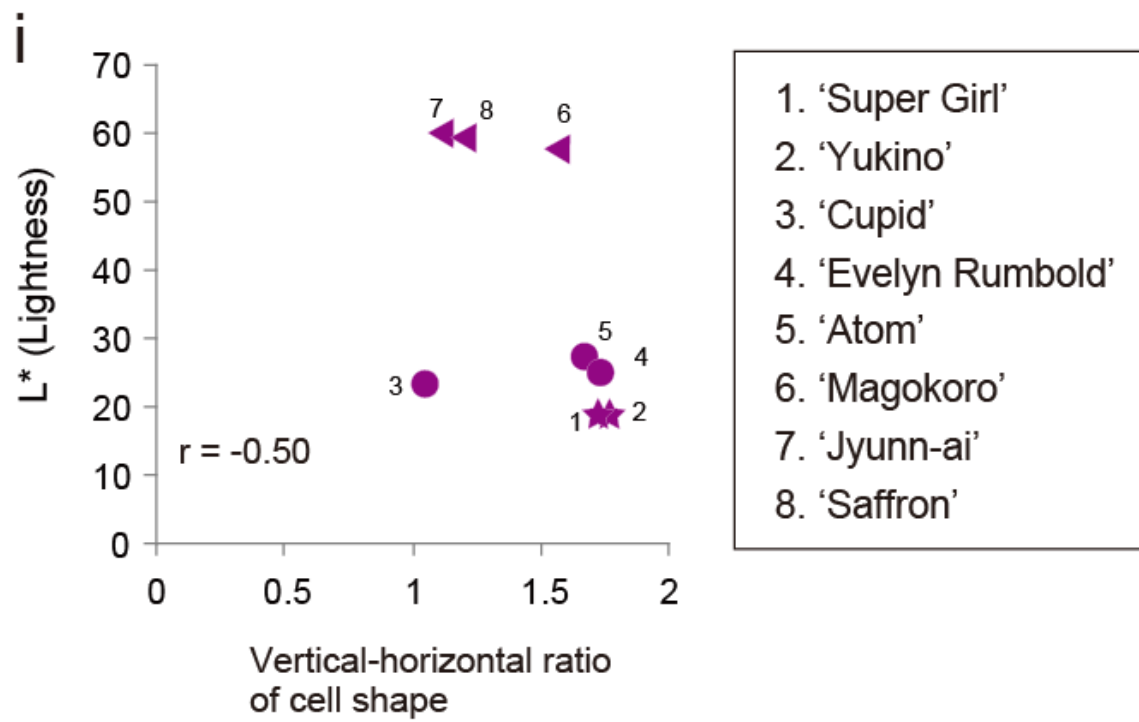
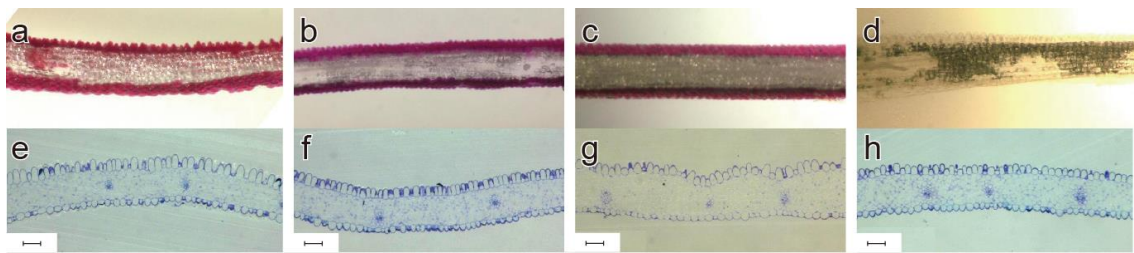


Fig. S2

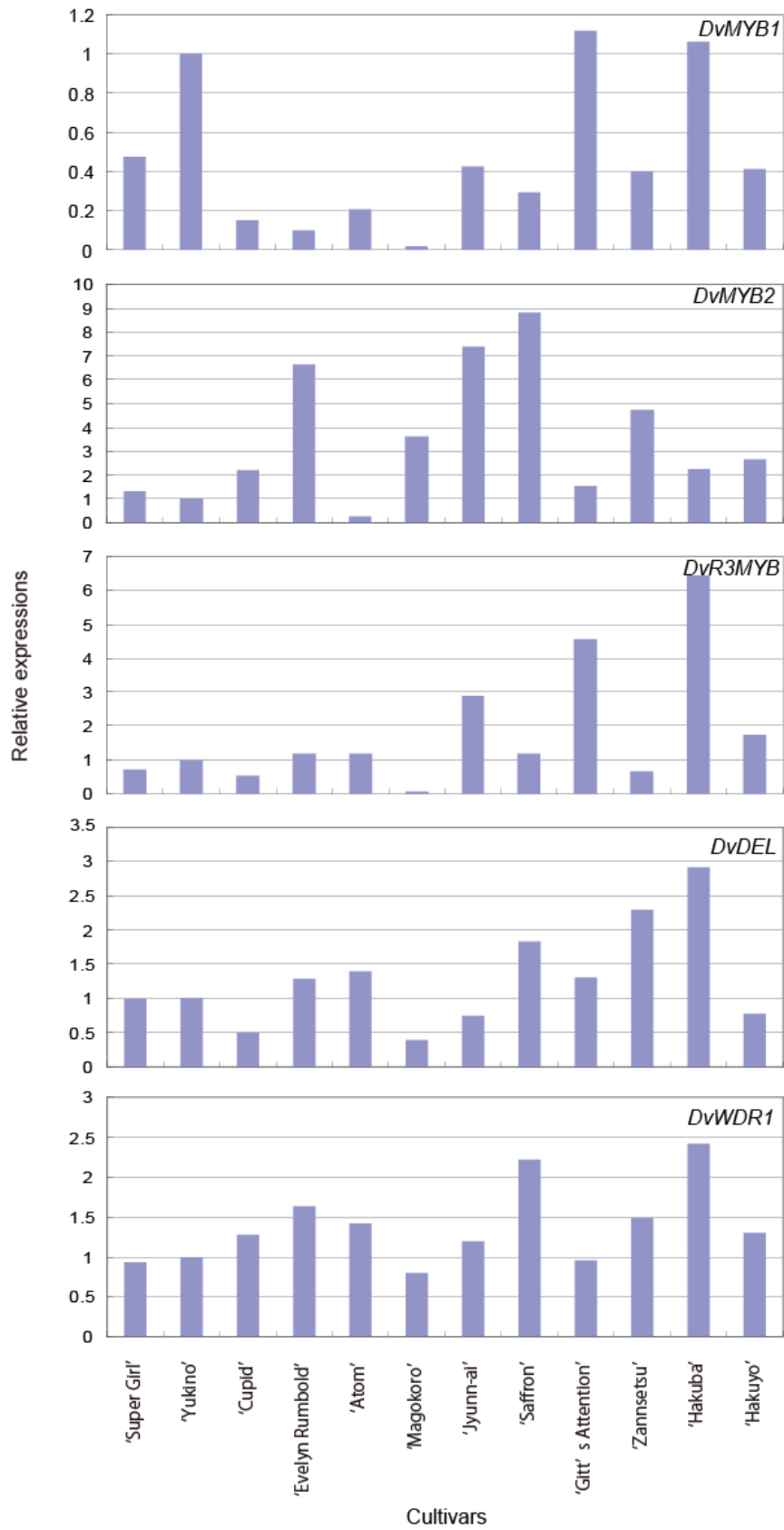


Fig. S3

```

mRNA-1 MFDIEREETIMAAAGSVNDDGLKEMLSAVQSVQWYI I IWQFCPERRVLVWGDGYNGA
mRNA-3 MFDIEREETIMAAAG-----LKEMLSAVQSVQWYI I IWQFCPERRVLVWGDGYNGA
mRNA-4 MFDIEREETIMAAAG-----LKEMLSAVQSVQWYI I IWQFCPERRVLVWGDGYNGA
mRNA-2 MFYLEREETIMAAAGPVNDDGLKEMLSAVQSVQWYI I IWQFCPERRVLVWGDGYNGA
** : :***** . *****:*****

mRNA-1 IKTRKTVPVEVSTEEAALSRSEQLRELYDSLASGEQQVAENQQAATVRRPSVALSPEDL
mRNA-3 IKTRKTVPVEVSTEEAALSRSEQLRELYDSLASGEQQVAESQQAATVRRPSVALSPEDL
mRNA-4 IKTRKTVPVEVSTEEAALSRSEQLRELYDSLASGEQQVTENQQAATVRRPSVALSPDDL
mRNA-2 IKTRKTVPVEVSTEEAALSRSEQLRELYDSLASGEQQVTENQQAATVRRPSMALSPEDL
*****:*.*****:****:*

mRNA-1 TEAEWFYLMCVSFSFPPGVGLVGEAYAKQDDLWLNAGNEVDSKVFTRAILAKSAYIQTVI
mRNA-3 TEAEWFYLMCVSFSFPPGVGLVGEAYAKQDDLWLNAGNEVDSKVFTRAILAKSAYIQTVI
mRNA-4 TEAEWFYLMCVSFSFPPGVGLVGEAYAKQDDLWLNAGNEVDSKVFTRAILAKSAYIQTVI
mRNA-2 TEAEWFYLMCVSFSFPPGVGLVGEAYAKQDDLWLNAGNEVDSKVFTRAILAKSAYIQTVI
*****:*****

mRNA-1 CIPVLNGVLELGTTEKVEETNEF IQHVKLFMTGNDNIMHPPKPTLSAHSNTTFSHQ
mRNA-3 CIPVLNGVLELGTTEKVEETNEF IQHVKLFMTGNNIMHLPKPTLSAHSNTTFSHQ
mRNA-4 CIPVLNGVLELGTTEKVEETNEF IQHVKLFMTGNDNIMHLPKPTLSAHSNTTFSHQ
mRNA-2 CIPVLNGVLELGTTEKVEETNEF IQHVKLFMTGNDNMHLPKPTLSAHSNTTFSHQ
*****:*.*****:*****

mRNA-1 TPDTIKLPDNTYSMDEGDDEEEEE-----DDDDDE-----AEDVGDEDENGTDFMKET
mRNA-3 TPDTIKLPDNTYSMDEGDDEEEEEEDDDDDDE-----GEDVGDEDENGTDFMKET
mRNA-4 TPDTIKLPDNTYSMDEGDDEEEEEEDDEGEDAGCDEAEDVGDEDENGTDFMKET
mRNA-2 TPDTIKLPDNTYSMDEGD-----DDDDDEGEDAGCDEAEDVGDEDENGTDFMKET
*****:*****

mRNA-1 YHVSSLQVPHNPKDSMVAFTETDELLQLGMSPDIKFGSPNDDSNLDSHFNLLATSLDSDS
mRNA-3 YHVSSQVPHNPKDSMVAFTETDELLQLGMSPDIKFGSPNDDSNLDSHFNLLATSLDSDS
mRNA-4 YHVSSQVPHNPKDSMVAFTETEELLQLGMSPDIKFRSPNDDSNLDSHFNLLATSLDSDS
mRNA-2 YHVSSQVPHNPKDSVVAFTETDELLQLGMSPDIKFGSPNDDSNLDSHFNLLATSLDSDS
*****:*****:*****:*****

mRNA-1 YRAVSTPGWSDNFELHNPSNIQLHTSEEFAPFTRYSDTLSTILHKQSTRWSSDTPSQH
mRNA-3 YRAVSTPGWSDNFELHNPSNIQLRTSEEFAPFTRYSDTLSTILHKQSTRWSSDTPSQH
mRNA-4 YRAVSTPGWSDNFELHNPSNTQLHTSEEFAPFTRYSDTLSTILHKQSTRWSSDTPSQH
mRNA-2 YRAVSTPGWSDNFELHNPSNIQLHT-SEFAPFTRYSDTLSTILHKQSTQWSSHTPLHH
*****:*****:*****:*****:*****

mRNA-1 NSPQSSFTTWTSTRHHSLLLPSSTTSQRILKYILFVFPFLYP-TATTTTISDSIASRLG
mRNA-3 NSPQSSFTTWTSTRHHSLLLPSSTTSQRILKYILFVFPFLYTTTTTTTISDSIASRLR
mRNA-4 NSPQSSFTTWTSTRHHSLLLPSSTTSQRILKYILFVFPFLYTTTTTTTISDSIASRLR
mRNA-2 NSPQSSFTTWTSTRHHSLLLPSSTTSQRILKYILFVFPFLY--TTTTTISDSIASRLR
*****:*****:*****:*****

Basic Helix Loop Helix
mRNA-1 KTTSHEELSANHVAERRRREKLNRF IILRTL VPLVTKMDKAS I LGDT IEYVKQLRNKV
mRNA-3 KTTSHEELSANHVAERRRREKLNRF IILRTL VPLVTKMDKAS I LGDT IEYVKQLRNKV
mRNA-4 KTTSHEELSANHVAERRRREKLNRF IILRTL VPLVTKMDKAS I LGDT IEYVKQLRNKV
mRNA-2 KTTSHEELSANHVAERRRREKLNRF IILRTL VPLVTKMDKAS I LGDT IEYVKQLRNKV
*****:*****

QDLETRCRLDNNSKVADKRKVRVVEHGNGGGGRAAVAVQVEVS I ENDALVEMQCKNRDG
mRNA-1 QDLETRCRLDNNSKVADKRKVRVVEHGNGGGGRAAVAVQVEVS I ENDALVEMQCKNRDG
mRNA-3 QDLETRCRLDNNSKVADKRKVRVVEHGNGGGGRAAVAVQVEVS I ENDALVEMQCKNRDG
mRNA-4 QDLETRCRLDNNSKVADKRKVRVVEHGNGGGGRAAVAVQVEVS I ENDALVEMQCKNRDG
mRNA-2 QDLETRCRLDNNSKVADKRKVRVVEHGNGGGRTAVAVQVEVS I ENDALVEMQCRQRDG
*****:*****:*****:*****

LLLLVMKKLREL.GVEITTVQSCVDGGMLNAEMRAKVKVKKGNNGRK I S I TQVKAIDQ I I
mRNA-1 LLLDVMKKLREL.GVEITTVQSCVDGGMLNAEMRAKVKVKKGNNGRK I S I TQVKAIDQ I I
mRNA-3 LLLDVMKKLREL.GVEITTVQSCVDGGMLNAEMRAKVKVKKGNNGRK I S I TQVKAIDQ I I
mRNA-4 LLLDVMKKLREL.GVEITTVQSCVDGGMLTAEARAKVKVKKGNNGRK I S I TQVKAIDQ I I
mRNA-2 *****:*****:*****:*****

SPL
mRNA-1 SPL
mRNA-3 SPL
mRNA-4 SPL
mRNA-2 SPL
***

```